



Patrick et al., 1989), with phase variation of LOS epitopes occurring at high frequency (Kimura & Hansen, 1986; Kimura et al., 1987; Weiser et al., 1989). These characteristics suggest that variation of LOS surface structures may be an important mechanism for Hib evasion of host defense mechanisms.

Like neisserial LOS, the LOS of *H. influenzae* consist of an oligosaccharide ketosidically linked via one or more 3-deoxy-D-manno-octulosonic acid (KDO) residues to a Lipid A moiety. Previous compositional studies have shown that *H. influenzae* LOS contain glucose, galactose, and L-glycero-D-manno-heptose as common sugar constituents, in addition to glucosamine and galactosamine in some strains (Fletcher & Insel, 1978; Inzana et al., 1985; Parr & Bryan, 1984; van Alphen et al., 1990; Zamze & Moxon, 1987). The KDO residue present in *H. influenzae* LOS has been found to be phosphorylated in both a recombinant (Helander et al., 1988) and a nontypable strain (Phillips et al., 1992). Structural heterogeneity observed in *H. influenzae* LOS has been associated with the oligosaccharide moieties (Campagnari et al., 1987; Patrick et al., 1987), which contain both strain specific and conserved epitopes. LOS from *Neisseria gonorrhoeae*, *Neisseria meningitidis*, and *Haemophilus ducreyi* have been found to share common epitopes with *H. influenzae* LOS, and recent studies have shown that some of these shared epitopes resemble host carbohydrate antigens (Campagnari et al., 1990; Mandrell et al., 1988; Virji et al., 1990) and are partially sialylated (Mandrell et al., 1991, 1992).

In this report, we describe the preliminary structural characterization of the LOS from Hib strain A2. DNA from this Hib strain was recently used to construct a genomic library in the  $\lambda$  bacteriophage EMBL3 (Spinola et al., 1990). Clones produced in this study expressed an Hib LOS oligosaccharide epitope in *Escherichia coli*. One clone, designated EMBLOS-1, appeared to produce a LOS with a 1.4-kDa oligosaccharide added to the 4.1-kDa lipopolysaccharide of the *E. coli* strain which was transfected. Monoclonal antibody (MAb) 6E4, which recognizes a stable epitope on two components in the Hib A2 LOS mixture, also recognized the novel 5.5-kDa component in the chimeric LOS. The chemical structure of this Hib epitope has not yet been elucidated, although a hexasaccharide from a nontypable strain of *H. influenzae* which also expresses the epitope was recently described (Phillips et al., 1992). The preliminary Hib A2 LOS structures described here share common features with the LOS from the nontypable strain but contain more highly branched carbohydrate structures. Genetic studies have suggested that the Hib A2 LOS may express the 6E4 epitope on a separate oligosaccharide branch from the phase-varying epitopes (McLaughlin et al., 1992). The partial LOS structures described here provide a structural basis for this hypothesis.

## EXPERIMENTAL PROCEDURES

### Materials

LPS from *Salmonella typhimurium* TV119 Ra mutant, galactose, glucose, galactosamine, glucosamine, 3-deoxy-D-manno-octulosonic acid (KDO), and anhydrous hydrazine were all obtained from Sigma (St. Louis, MO). Aqueous HF (48%) was purchased from Mallinckrodt (Muskegon, MI). Water (18 M $\Omega$ ) required for the Dionex chromatography was generated from deionized water using a Millipore Milli-Q water purification system. All other reagents and solvents used were of reagent grade.

### Methods

**Isolation of LOS from Hib Strain A2.** Hib strain A2 was isolated from the cerebrospinal fluid of an Alaskan child as previously described (Spinola et al., 1990). LOS from this Hib strain was prepared by the extraction procedure of Darveau and Hancock (1983).

**O-Deacylation of LOS.** Hib A2 LOS (1.7 mg) was O-deacylated by treatment with anhydrous hydrazine following the procedure of Helander et al. (1988) as previously described (Phillips et al., 1992).

**Neuraminidase Treatment of O-Deacylated LOS.** A portion of the O-deacylated A2 LOS sample ( $\approx 50$   $\mu$ g) was treated with 50 milliunits of neuraminidase (Sigma Type VI) in 50  $\mu$ L of PBS, pH 6.0, for 2 h at 37 °C. The enzyme digest was desalted by microdialysis against H<sub>2</sub>O (Pierce, microdialyzer system 500) using a 1000 MW cutoff membrane (Spectra/Por). The retentate was lyophilized and later redissolved in H<sub>2</sub>O for mass spectral studies.

**Isolation and Purification of Oligosaccharide and Lipid A Fractions.** The LOS from Hib strain A2 (14 mg) and commercially available *Salmonella typhimurium* TV 119 Ra mutant (20 mg) were hydrolyzed in 1% acetic acid (2 mg of LOS/mL) for 2 h at 100 °C. The hydrolysates were centrifuged at 5000g for 20 min at 4 °C and the supernatants removed. Pellets were washed with 1–3 mL of H<sub>2</sub>O and centrifuged again (5000g, 20 min, 4 °C). The supernatants and washings were pooled and lyophilized to give the oligosaccharide fractions. The Lipid A pellets were partitioned in CHCl<sub>3</sub>/methanol/0.1 N HCl (2/1/2 v/v/v), and the organic layers plus emulsion layers were combined and evaporated to dryness.

The Hib A2 oligosaccharide fraction (7.0 mg) was dissolved in 0.3 mL of 0.05 M pyridinium acetate buffer (pH 5.2), centrifuge-filtered through a 0.45- $\mu$ m Nylon-66 membrane (Microfilterfuge tube, Rainin), and applied to two Bio-Gel P-4 columns connected in series (1.6  $\times$  79 cm and 1.6  $\times$  76.5 cm, <400 mesh; Bio-Rad). The columns were equipped with water jackets maintained at 30 °C. Upward elution at a flow rate of  $\approx 10$  mL/h was achieved with a P-1 peristaltic pump (Pharmacia), and fractions were collected at 10-min intervals and evaporated to dryness in a Speed-Vac concentrator. A refractive index detector (Knauer) was used to monitor column effluent, and chromatograms were recorded and stored with a Shimadzu C-R3A Chromatopac integrator.

**Dephosphorylation of Oligosaccharides.** Oligosaccharides were placed in 1.5-mL polypropylene tubes and treated with cold 48% aqueous HF to make 5–10  $\mu$ g/ $\mu$ L solutions. Samples were kept for 16–24 h at 4 °C and then aqueous HF was evaporated as previously described (Phillips et al., 1992).

**Monosaccharide Composition Analysis.** For composition analysis, dephosphorylated oligosaccharide fractions were dissolved in 200  $\mu$ L of H<sub>2</sub>O, treated with 200  $\mu$ L of 4 M trifluoroacetic acid, and heated for 4.5 h at 100 °C. The hydrolysates were evaporated to dryness in a Speed-Vac concentrator, redissolved in 20  $\mu$ L H<sub>2</sub>O, and dried again. Hydrolysates were analyzed by high-performance anion-exchange chromatography with pulsed amperometric detection (Hardy et al., 1988) using the Dionex BioLC system (Dionex, Sunnyvale, CA) described previously (Phillips et al., 1992). Monosaccharides were separated on a CarboPac PA1 column (4  $\times$  250 mm) using the following gradient: (1) 16 mM NaOH for 20 min, (2) linear to 40 mM NaOH in 10 min, (3) linear to 100 mM NaOH and 100 mM NaOAc in 5 min, and (4) linear to 160 mM NaOAc in 15 min while holding 100 mM

NaOH constant. Response factors for the various monosaccharides were determined with a standard monosaccharide mixture containing GalNH<sub>2</sub>, GlcNH<sub>2</sub>, Gal, Glc, and KDO. Approximately 10 nmol of the dephosphorylated oligosaccharide from *S. typhimurium* Ra mutant was hydrolyzed under the same conditions to provide authentic L-glycero-D-manno-heptose.

**Methylation Analysis.** Linkage analysis was performed using the microscale method of Levery and Hakomori (1987) modified for use with powdered NaOH (Larson et al., 1987). Given the resistance of Hep–Hep bonds to acid hydrolysis, the longer hydrolysis times (21 h) and slightly greater acidic conditions of the older Hakomori procedure (Stellner et al., 1973) were used. Details of this procedure have been reported elsewhere (Phillips et al., 1992). Partially methylated alditol acetates were analyzed by GC/MS in the EI and CI modes on a VG70SE mass spectrometer as described previously (Phillips et al., 1990).

**Derivatization of Oligosaccharides with Butyl Phenylhydrazine and HPLC Purification.** Oligosaccharide fractions ( $\approx 100 \mu\text{g}$ ) dissolved in 10  $\mu\text{L}$  of H<sub>2</sub>O were placed in 1-mL glass Reacti-Vials. Approximately 3 molar equiv of BPH in 40  $\mu\text{L}$  of methanol was added to each sample, followed by  $\approx 0.5 \mu\text{L}$  of glacial acetic acid. The reaction mixtures were heated at 80 °C for 30 min, cooled, and then dried under a stream of N<sub>2</sub>. The samples were redissolved in H<sub>2</sub>O and separated by HPLC using a Vydac C-18 column (25 cm  $\times$  4.6 mm i.d.). The BPH-oligosaccharide derivatives were eluted with a linear gradient of H<sub>2</sub>O to 50% CH<sub>3</sub>CN in 50 min at a flow rate of 1 mL/min. Both HPLC solvents contained 0.05% trifluoroacetic acid. The derivatives were detected at 335 nm with a Kratos 783 variable-wavelength detector.

**Liquid Secondary Ion Mass Spectrometry.** LSIMS was performed using a Kratos MS50S mass spectrometer with a cesium ion source (Falick et al., 1986). Oligosaccharide samples (in 1  $\mu\text{L}$  of H<sub>2</sub>O) were added to 1  $\mu\text{L}$  of glycerol/thioglycerol (1/1) on a stainless steel probe tip and Lipid A samples (in 1  $\mu\text{L}$  of CHCl<sub>3</sub>) were run in 1  $\mu\text{L}$  of nitrobenzyl alcohol/triethanolamine (1/1). A Cs<sup>+</sup> ion primary beam energy of 10 keV was used and the secondary sample ions were accelerated to 8 keV. Scans were taken in the negative-ion mode at 300 s/decade and recorded with a Gould ES-1000 electrostatic recorder. The spectra were mass-calibrated manually with Ultramark 1621 (PCR Research Chemicals, Inc., Gainesville, FL) to an accuracy of better than  $\pm 0.2$  Da.

Tandem mass spectrometry (MS/MS) was performed using a four-sector mass spectrometer (Kratos Concept II HH, Kratos Analytical, Manchester, England) equipped with a 4% diode array detector on MS-II as previously described (Walls et al., 1990). Spectra were taken in the negative-ion mode using a Cs<sup>+</sup> beam energy of 18 keV. The isotopically pure <sup>12</sup>C component of the parent deprotonated molecular ion was collisionally activated with helium and the collision cell was floated at a potential of 2 kV, resulting in a collision energy of 6 keV. The mass scales on MS-I and MS-II were both calibrated with CsI using a Kratos Mach 3 data system as previously described (Walls et al., 1990).

**Electrospray Mass Spectrometry.** Samples were analyzed on a Bio-Q mass spectrometer (VG Instruments, Manchester, England) with an electrospray ion source operating in the negative-ion mode. The electrospray tip voltage was typically 4.0 kV. O-Deacylated LOS samples were dissolved in H<sub>2</sub>O and 1–3  $\mu\text{L}$  aliquots were injected via a Rheodyne injector into a stream of H<sub>2</sub>O/acetonitrile (1/1 v/v) containing 1% acetic acid. A flow rate of 2–4  $\mu\text{L}/\text{min}$  was maintained with

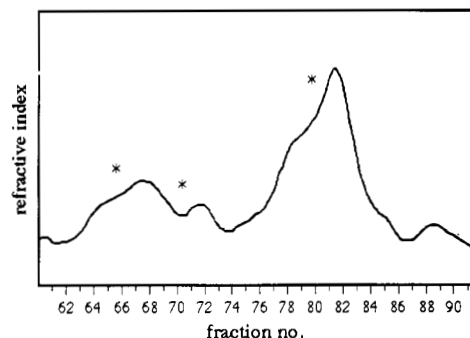


FIGURE 1: Bio-Gel P-4 column separation of the oligosaccharides from Hib strain A2. Oligosaccharides were detected with a refractive index detector. The elution volume of the major peak was  $\approx 155$  mL, and  $V_0$  and  $V_i$  for the column were  $\approx 80$  and 280 mL, respectively. The LSIMS spectra of fractions marked with asterisks are shown in Figure 2.

a  $\mu\text{LC}$ -500 syringe pump (Isco, Lincoln, NE). Mass calibration was carried out with an external horse heart myoglobin reference using the VG Bio-Q software, and the instrument was tuned up in the negative-ion mode with sulfated cholecystinin-8 (Peninsula Laboratories).

## RESULTS

**Molecular Weight Analysis of Oligosaccharide and Lipid A Components.** The LOS mixture produced by Hib strain A2 was shown by sodium dodecyl sulfate–polyacrylamide gel electrophoresis (SDS–PAGE) to consist of seven to eight glycolipid bands, ranging in size from approximately 3.1 to 4.5 kDa (McLaughlin et al., 1992). This mixture was considerably more heterogeneous than the LOS derived from the *H. influenzae* nontypable strain 2019 examined previously (Phillips et al., 1992). As a first step in the structural characterization of these glycolipids, the LOS mixture was subjected to mild acid hydrolysis to produce separate oligosaccharide and Lipid A fractions. As expected from the SDS–PAGE profile, a complex mixture of oligosaccharides was obtained, as evident from the separation by size-exclusion chromatography (Figure 1). The molecular weights of oligosaccharides in fractions 62–89 were determined by LSIMS in the negative-ion mode. Figure 2 shows the LSIMS spectra of three selected column fractions, and Table I lists all of the major molecular ions detected in the fractions analyzed. As indicated, a partial separation of components based on their molecular size was achieved. Clearly, a major component of the mixture found in the largest peak (fractions 77–83) was the species with a deprotonated molecular ion,  $(M - H)^-$ , at  $m/z$  1566.5 ( $M_r$  1567.5).<sup>2</sup> Major higher molecular weight components were observed at  $m/z$  1890.6, 1931.7, and 2052.6. In preliminary analyses, it was noted that many of the molecular ions observed in the Hib A2 mixture were present as minor components in the oligosaccharides derived from *H. influenzae* nontypable strain 2019 (Phillips et al., 1992).

Proposed compositions for the majority of the molecular ions observed (Table II) were derived by combination of common oligosaccharide structural moieties such as hexose (Hex), *N*-acetylhexosamine (HexNAc), heptose (Hep), 3-deoxy-D-manno-octulosonic acid (KDO), phosphate (P),

<sup>2</sup> All oligosaccharide and Lipid A ions measured by LSIMS are reported as either monoisotopic or nominal masses of the <sup>12</sup>C-containing component. O-Deacylated LOS molecular ions observed by ESMS are reported as their average masses.

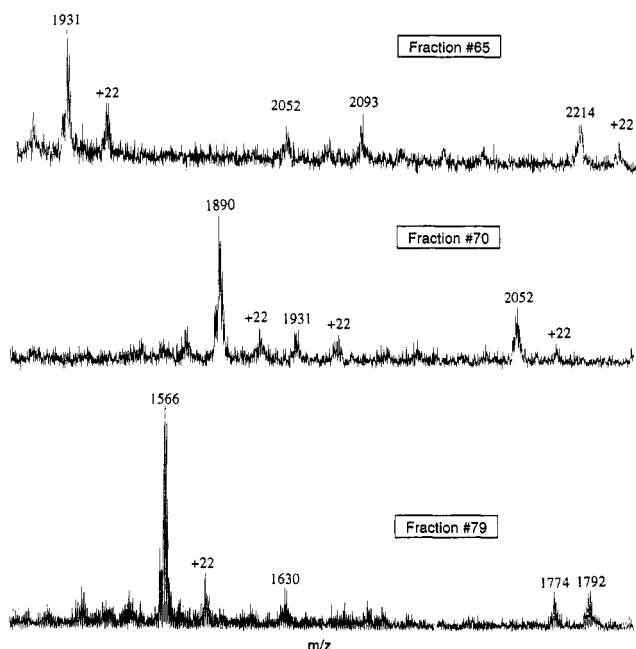


FIGURE 2: Partial negative-ion LSIMS spectra of three oligosaccharide fractions from the Bio-Gel P-4 column. Peaks labeled as +22 Da are sodiated species,  $(M - 2H + Na)^-$ .

Table I: Molecular Ions Observed in the Hib A2 Oligosaccharide Fractions<sup>a,b</sup>

fraction	molecular ions, $(M - H)^-$
62, 63	2093.8
64	2214.8, 2093.9
65, 66	2214.8, 2093.9, 2052.9, <b>1931.8</b>
67	2139.2, 2052.6, <b>1931.7</b>
68	2117.7, <b>2052.6</b> , <b>1931.7</b> , 1890.7
69, 70	2052.7, 1931.7, 1890.7
71	1890.6
72	<b>1890.6</b> , 1728.7
73	1890.6, 1792.8, <sup>c</sup> 1728.7
74, 75	1792.6, <sup>c</sup> 1728.5, 1566.5
76	<b>1792.7</b> , <sup>c</sup> 1728.7, 1630.6, <sup>c</sup> 1566.6
77	<b>1792.6</b> , <sup>c</sup> 1730.5, 1630.7, <sup>c</sup> <b>1566.5</b>
78	1792.4, <sup>c</sup> 1774.4, <sup>d</sup> <b>1566.4</b> , 1404.4, 1242.3
79	1792.7, <sup>c</sup> 1774.7, <sup>d</sup> 1630.6, <sup>c</sup> <b>1566.5</b> , 1404.3
80	1774.5, <sup>d</sup> 1630.6, <sup>c</sup> <b>1566.5</b> , 1523.5, 1404.5, 1242.1
81	1896.6, 1774.3, <sup>d</sup> 1682.6, 1574.4, <b>1566.4</b> , 1404.4
82	1774.5, <sup>d</sup> <b>1566.4</b> , 1404.2, 1242.4
83	1774.5, <sup>d</sup> <b>1566.6</b> , <b>1404.5</b> , 1242.4
84	1566.6, <b>1404.6</b> , 1242.2
85	1614.4, 1566.4, 1468.3, <sup>c</sup> <b>1404.2</b> , 1242.3
86, 87	1612.5, <sup>d</sup> 1566.4, <b>1404.6</b> , <b>1242.4</b>
88	1612.5, <sup>d</sup> 1450.5, <sup>d</sup> <b>1404.6</b> , <b>1242.4</b>
89	1450.5, <sup>d</sup> <b>1404.6</b> , <b>1242.5</b>

<sup>a</sup> Ions in bold face type represent the most abundant species. <sup>b</sup> In addition to  $(M - H)^-$  ions, +226 Da (<sup>c</sup>) and +208 Da (<sup>d</sup>) adduct ions were also observed, which could be suppressed by acidification of the LSIMS matrix (Phillips et al., 1992).

phosphoethanolamine (PEA), pyrophosphoethanolamine (PPEA), and sialic acid (NANA).<sup>3,4</sup> As in *H. influenzae* nontypable strain 2019 (Phillips et al., 1992) and *H. ducreyi* strain 35000 (Melaugh et al., 1992), the Hib A2 oligosac-

Table II: Molecular Weights and Compositions of Oligosaccharide Components from Hib A2 LOS<sup>a</sup>

$(M - H)^-$	$M_r$	proposed compositions
2214.8	2215.8	8 Hex, 3 Hep, PEA, KDO*
2093.9	2094.9	6 Hex, 3 Hep, HexNAc, PEA, KDO*
2052.6	2053.6	7 Hex, 3 Hep, PEA, KDO*
1931.7	1932.7	5 Hex, 3 Hep, HexNAc, PEA, KDO*
1890.6	1891.6	6 Hex, 3 Hep, PEA, KDO*
1728.5	1729.5	5 Hex, 3 Hep, PEA, KDO*
1566.5	1567.5	4 Hex, 3 Hep, PEA, KDO*
1523.5	1524.5	4 Hex, 3 Hep, P, KDO*
1404.5	1405.5	3 Hex, 3 Hep, PEA, KDO*
1242.4	1243.4	2 Hex, 3 Hep, PEA, KDO*

<sup>a</sup> KDO\* stands for anhydro-KDO.

charide structures appeared to contain a Hep<sub>3</sub>(anhydro-KDO) core. The anhydro-KDO moiety (KDO - 18 Da) is believed to arise as an artifact of the hydrolysis procedure via the  $\beta$ -elimination of phosphate from the 4-position of KDO (Auzanneau et al., 1991).

The presence of one PEA group on all of the major oligosaccharides was confirmed by dephosphorylating selected fractions by treatment with aqueous HF. When analyzed by LSIMS, all of the species proposed to contain PEA lost a 123-Da moiety after the HF treatment, consistent with the presence of one PEA. In cases where proposed compositions could include either a HexNAc or an additional PPEA group, both of which have the same residue mass of 203 Da, the HF treatment clearly established the presence of the HexNAc moiety. Thus, the molecular weight data suggest that only the higher mass components of the Hib A2 oligosaccharide mixture contain HexNAc.

The Lipid A fraction was also analyzed by LSIMS and the spectrum obtained contained  $(M - H)^-$  ions for both a diphosphorylated ( $m/z$  1823) and a monophosphorylated ( $m/z$  1743) species, consistent with the previously described Lipid A preparations from *H. influenzae* (Helander et al., 1988; Phillips et al., 1992) and *H. ducreyi* 35000 (Melaugh et al., 1992). Fragment ions corresponding to the loss of myristic acid ( $m/z$  1595 and 1515) and elimination of a myristoxymyristol group as a ketene ( $m/z$  1387 and 1307) were the most abundant fragments in the spectrum. These data are consistent with a Lipid A composed of a glucosamine disaccharide bearing four 3-hydroxymyristic acids, two myristic acids, and two phosphate groups. The monophosphorylated Lipid A present in the preparation is believed to result from partial loss of reducing terminal phosphate during either the acid hydrolysis step or the extraction procedure. This phosphate moiety is known to be somewhat acid-labile (Helander et al., 1988).

**Analysis of O-Deacylated LOS by Electrospray Mass Spectrometry (ESMS).** A method of evaluating "intact" LOS samples without chemical cleavage of the oligosaccharide from the Lipid A has been developed using electrospray mass spectrometry (Gibson et al., 1993). To make the amphipathic LOS suitable for ESMS analysis, samples are first O-deacylated with anhydrous hydrazine. This treatment removes O-linked fatty acids from the Lipid A moiety (and O-linked acetate groups from the carbohydrate moiety, if present) but does not affect acid-labile moieties. In combination with independent analyses of the oligosaccharide and Lipid A moieties, mass spectral analysis of O-deacylated LOS samples provides a more complete picture of the intact glycolipids.

Figure 3A shows the negative-ion ESMS spectrum of the O-deacylated LOS from Hib strain A2. The spectral region shown includes both doubly,  $(M - 2H)^{2-}$ , and triply,  $(M -$

<sup>3</sup> Residue mass values (monoisotopic mass, average mass) for LOS structural moieties are as follows: Hex (162.053, 162.145), Hep (192.063, 192.172), HexNAc (203.079, 203.198), KDO (220.058, 220.182), NANA (291.095, 291.262), phosphate (79.966, 79.980), PEA (123.008, 123.050), PPEA (202.975, 203.030). The average molecular mass of the diphosphorylated O-deacylated Lipid A is 953.029 Da.

<sup>4</sup> A computer algorithm was used to determine oligosaccharide compositions from molecular weight data (W. Hines, University of California, San Francisco).

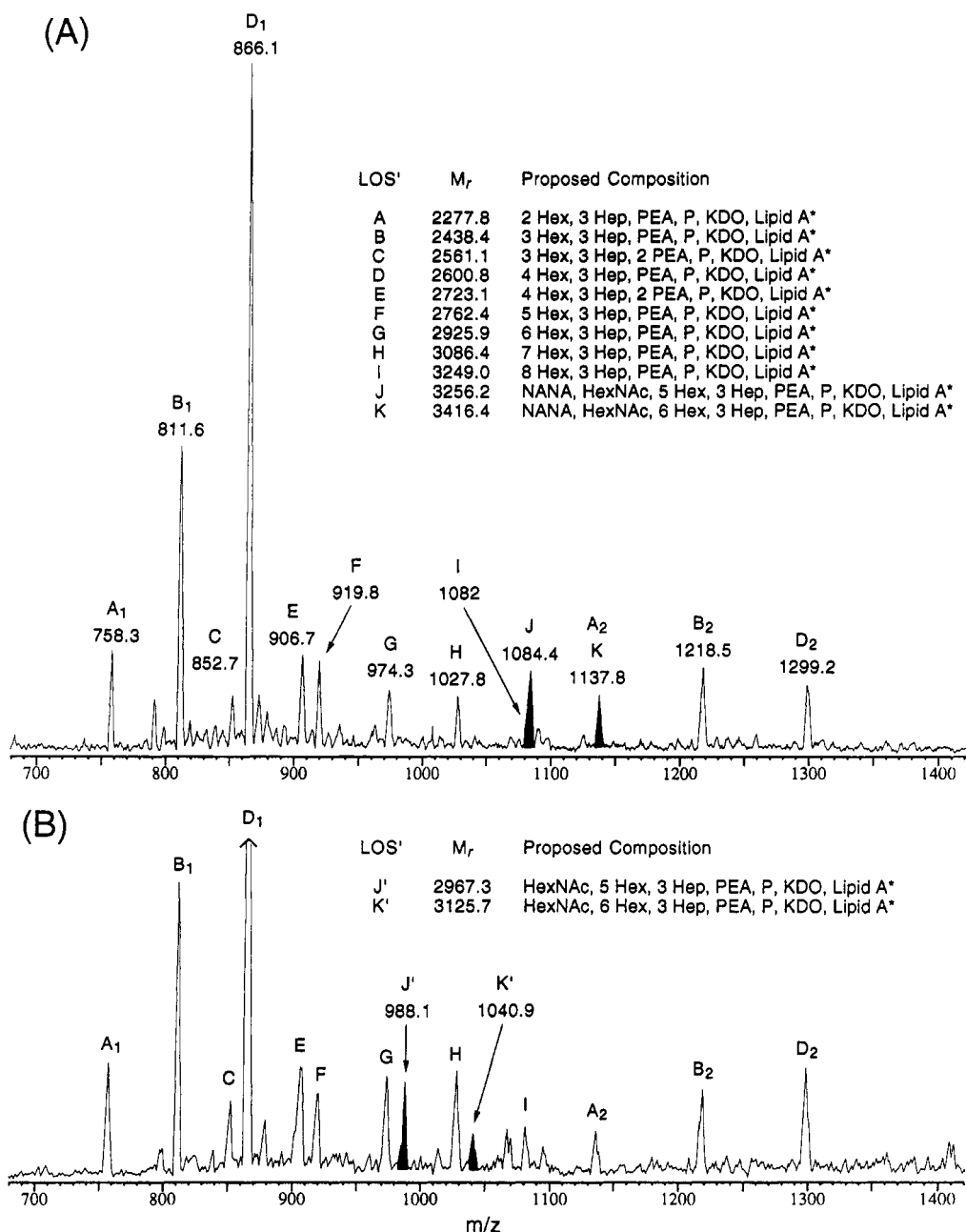


FIGURE 3: Negative-ion electrospray mass spectra of the O-deacylated LOS from Hib strain A2 before (A) and after (B) treatment with neuraminidase. The spectral region shown includes both doubly,  $(M - 2H)^{2-}$ , and triply,  $(M - 3H)^{3-}$ , charged ions. Components are identified by letters and subscripts denote different multiply charged ions arising from the same species. In both spectra, mass measurements are accurate to within  $\pm 0.3$ – $0.5$  Da, leading to molecular mass measurements with accuracies on the order of  $\pm 1$ – $2$  Da. The shaded peaks are the components affected by the neuraminidase treatment. Peak  $D_1$ , which is shown truncated in spectrum B, was the base peak in both spectra. LOS' refers to O-deacylated LOS, and Lipid A\* stands for diphosphorylated O-deacylated Lipid A. Peaks at  $m/z$  1067.2, 1069.9, and 1095.1 in spectrum B are contaminants.

$3H)^{3-}$ , charged ions,<sup>2</sup> which can be assigned as arising from eleven separate components. The three ions at  $m/z$  1137.8, 1218.5, and 1299.2 are doubly charged counterparts of the triply charged ions at  $m/z$  758.3, 811.6, and 866.1, respectively. These three pairs of ions arise from O-deacylated LOS of  $M_r$  2277.8, 2438.4, and 2600.8. Alternatively, the ion at  $m/z$  1137.8 could also be assigned as a triply charged species arising from an O-deacylated LOS of  $M_r$  3416.4. The remaining major ions in the spectrum at  $m/z$  852.7, 906.7, 919.8, 974.3, 1027.8, 1082, and 1084.4 are all triply charged species, corresponding to O-deacylated LOS of  $M_r$  2561.1, 2723.1, 2762.4, 2925.9, 3086.4, 3249, and 3256.2, respectively. The peak at  $m/z$  1082 appears as a shoulder on the larger peak at  $m/z$  1084.4.

To arrive at proposed compositions for the O-deacylated LOS, one can assume a constant mass of 953.029 Da for diphosphorylated O-deacylated *H. influenzae* Lipid A and then add on the residue masses of the monosaccharides and phosphate esters.<sup>3</sup> To compare the experimental molecular weights of the O-deacylated LOS with those obtained from SDS-PAGE of intact LOS, the mass difference between intact *H. influenzae* Lipid A and the O-deacylated Lipid A must be taken into account. Table III lists the proposed compositions for the eleven major LOS species derived from Hib A2. As was the case for the O-deacylated LOS from *H. influenzae* nontypable strain 2019 and *H. ducreyi* strain 35000, the Hib A2 structures appear to contain only a single KDO residue linking the oligosaccharide to the Lipid A moiety. Most of

Table III: Observed and Calculated Molecular Weights of Hib A2 LOS and O-Deacylated LOS

observed $M_r$ for O-deacylated LOS	calculated $M_r$ for O-deacylated LOS	calculated $M_r$ for intact LOS	proposed LOS compositions
2277.8	2277.0	3150.5	2 Hex, 3 Hep, PEA, P, KDO, Lipid A
2438.4	2439.2	3312.7	3 Hex, 3 Hep, PEA, P, KDO, Lipid A
2561.1	2562.2	3435.7	3 Hex, 3 Hep, 2 PEA, P, KDO, Lipid A
2600.8	2601.3	3474.8	4 Hex, 3 Hep, PEA, P, KDO, Lipid A
2723.1	2724.4	3597.9	4 Hex, 3 Hep, 2 PEA, P, KDO, Lipid A
2762.4	2763.5	3636.9	5 Hex, 3 Hep, PEA, P, KDO, Lipid A
2925.9	2925.6	3799.1	6 Hex, 3 Hep, PEA, P, KDO, Lipid A
3086.4	3087.8	3961.2	7 Hex, 3 Hep, PEA, P, KDO, Lipid A
3249.0 <sup>a</sup>	3249.9	4123.4	8 Hex, 3 Hep, PEA, P, KDO, Lipid A
3256.2	3257.9	4131.4	NANA, HexNAc, 5 Hex, 3 Hep, PEA, P, KDO, Lipid A
3416.4	3420.1	4293.6	NANA, HexNAc, 6 Hex, 3 Hep, PEA, P, KDO, Lipid A

<sup>a</sup> The triply charged ion for this component was not well resolved in the original spectrum but was clearly defined in the spectrum of the neuraminidase-treated sample.

the species present belong to a series of related structures which contain one PEA group and differ primarily by the number of hexose residues. A smaller subpopulation of structures with two PEA groups also exists. Having already established the presence of two phosphates on the Lipid A and one PEA on the major A2 oligosaccharides, the "extra" phosphate present in these O-deacylated LOS must exist on the 4-position of KDO, a site from which phosphate groups are readily eliminated under mild acid hydrolysis conditions (Auzanneau et al., 1991). The  $(M - 3H)^{3-}$  ion at  $m/z$  1084.4 does not fit for a structure containing only Hex and Hep and would appear to represent a species containing 5 Hex, 3 Hep, 1 HexNAc, and 1 NANA residue. If the ion at  $m/z$  1137.8 is assigned as a triply charged species, it could represent a structure containing 6 Hex, 3 Hep, 1 HexNAc, and 1 NANA residue.

To confirm the presence of sialic acid in these two LOS components, the O-deacylated sample was treated with neuraminidase, desalted, and then analyzed again by electrospray mass spectrometry. The resulting spectrum (Figure 3B) clearly indicated that the two components proposed to contain sialic acid (components J and K) were no longer present in the mixture. In their place, new peaks for the desialylated structures appeared at  $(M - 3H)^{3-}$  988.1 and 1040.9, labeled as components J' and K', respectively. These peaks were shifted by the loss of the residue mass for sialic acid (calculated  $\Delta$  291.3 Da) and their masses fit for species containing 5 Hex, 3 Hep, and 1 HexNAc (component J') and 6 Hex, 3 Hep, and 1 HexNAc (component K'). The shifting of peak K permitted a more accurate mass assignment of peak A<sub>2</sub>, which was overlapping with peak K in the original spectrum. Additionally, the  $(M - 3H)^{3-}$  ion at 1082.0 in the neuraminidase-treated sample (peak I), which corresponds to an O-deacylated LOS of  $M_r$  3249.0, was not well resolved from peak J in the original spectrum. Due to the acid lability of sialic acid residues, it is not surprising that only the asialo structures resulting from components I and J were detected in the oligosaccharide fraction from Hib A2 LOS (see Table II).

**Monosaccharide Composition and Linkage Analysis.** Selected oligosaccharide fractions from the size-exclusion column were pooled and treated with further chemical analyses. To obtain precise monosaccharide compositions for the various fractions, small aliquots were taken and hydrolyzed in 2 M TFA for 4.5 h. The dephosphorylated oligosaccharide from *S. typhimurium* Ra mutant was hydrolyzed under the same conditions to provide a known standard. Table IV shows the relative molar ratios of monosaccharides obtained in the indicated column fractions, derived from comparison to the standard *S. typhimurium* Ra hydrolysate and normalized to 3.0 equiv of Hep in each fraction. As suggested by the LSIMS

Table IV: Monosaccharide Compositions of Hib A2 Oligosaccharide Fractions<sup>a</sup>

fractions	GlcNH <sub>2</sub>	Gal	Glc	Hep
63–64	0.7	3.4	4.4	3.0
67–68	0.5	2.5	4.3	3.0
71–72		2.1	4.6	3.0
75–76		1.8	4.7	3.0
80–81		0.3	5.6	3.0
84–85		0.1	4.3	3.0
88–89		0.1	3.5	3.0

<sup>a</sup> Hydrolysates were analyzed by high-performance anion-exchange chromatography with pulsed amperometric detection. Molar ratios were derived from comparison to the *S. typhimurium* hydrolysate of known composition and normalized to 3.0 Hep (L-glycero-D-manno-heptose) in each fraction.

analysis, composition analysis confirmed that only the higher molecular weight components of the Hib A2 oligosaccharide mixture contain HexNAc, which was shown to be exclusively GlcNAc. Although many of the fractions analyzed contain more than one major oligosaccharide structure, some of the lower molecular weight fractions (i.e., fractions 88–89, 84–85, and 80–81) contained one dominant species. Thus, composition analysis suggests that the oligosaccharides of  $M_r$  1243.4, 1405.5, and 1567.5 contain only glucose as their hexose components. Galactose only becomes an appreciable component in the fractions containing higher molecular weight structures.

To establish the glycosidic linkages present in the Hib A2 oligosaccharides, aliquots of the same fractions used for composition analyses were used for methylation analysis. The partially methylated alditol acetates (PMAAs) observed by GC/MS are listed in Table V. In general, the types of PMAAs detected in the various fractions are consistent with the monosaccharide compositions shown in Table IV. Most striking is the detection of two trlinked heptoses, suggesting two branch points in the oligosaccharide core. Furthermore, the PMAAs obtained from fractions 80–81 suggest that the dephosphorylated  $M_r$  1567.5 octasaccharide ( $M_r$  1444.5), which consists of 4 Glc, 3 Hep, and 1 anhydro-KDO, contains two terminal Glc and two 1,4-linked Glc. This simple composition limits the partial structures that are possible for this component to three alternative sequences, assuming that the heptose core linkages are analogous to those in *H. influenzae* nontypable strain 2019 (Phillips et al., 1992). To establish the correct sequence of this and other components in the Hib oligosaccharide mixture, further mass spectrometric studies were conducted.

**Oligosaccharide Sequencing.** Tandem mass spectrometry (MS/MS) in the negative-ion mode was used to select single

Table V: Methylation Analysis of Hib A2 Bio-Gel P-4 Column Fractions<sup>a</sup>

PMAAs <sup>b</sup>	fractions							
	63–64	67–68	71–72	75–76	77–78	80–81	84–85	88–89
1-Glc	1.1	1.4	1.1	2.4	2.1	4.0	2.6	3.2
1-Gal	3.4	2.9	2.5	1.5	1.0	0.3		
1,4-Gal	1.1	0.5	1.0	0.7	0.3			
1,4-Glc	6.9	7.8	5.0	4.8	2.7	4.6	2.2	2.4
1,3-Gal	1.2	0.8	0.2					
1-Hep	1.0	1.0	1.0	1.0	1.0	1.0	1.0	1.0
1,2-Hep				0.2	0.2		0.2	0.7
1,3,4-Hep	1.3	1.1	1.2	1.2	0.8	1.4	0.8	0.8
1,2,3-Hep	1.8	1.8	1.6	1.3	1.3	1.7	1.4	0.4
1,4-GlcNAc	0.3	0.3						

<sup>a</sup> Values are relative peak heights from the GC/MS EI total ion chromatograms, normalized to 1.0 terminal heptose. <sup>b</sup> In addition to these partially methylated alditol acetates, a trace amount of a 1,4,6-linked hexose was also detected in all of the fractions, which may result from undermethylation of the oligosaccharides or from a set of minor components with an additional branch point.

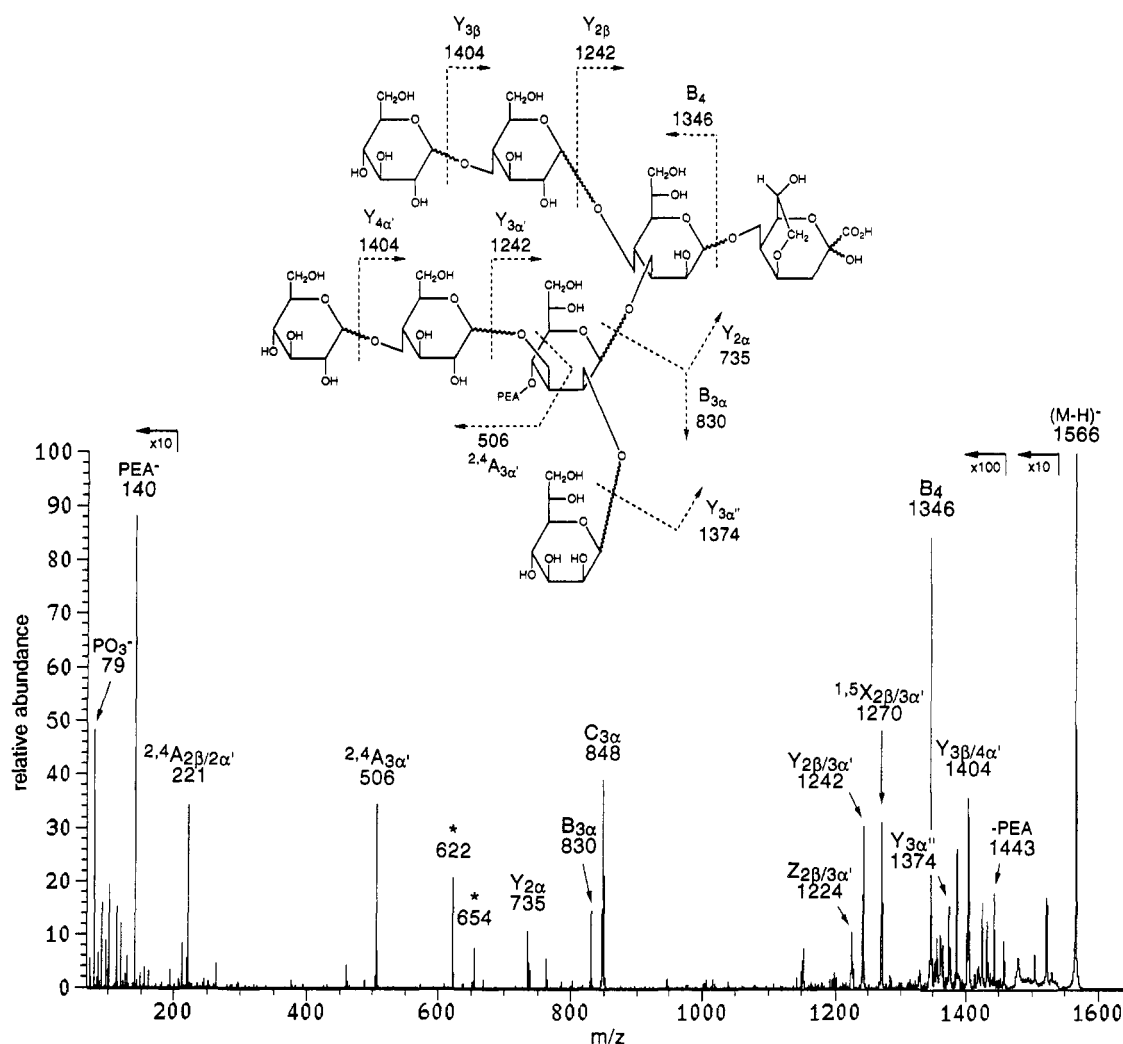


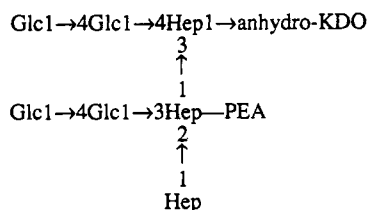
FIGURE 4: Negative-ion MS/MS spectrum of the octasaccharide at  $m/z$  1566.5. Fragments are labeled according to the nomenclature proposed by Domon and Costello (1988). The  $\alpha$  and  $\beta$  subscripts distinguish the major and minor branches, respectively. Additional ions present but not labeled on the spectrum include  $m/z$  1522 ( $-\text{CO}_2$ ), 1432 ( $^{1,5}\text{X}_{3\beta/4\alpha'}$ ), 1425 [ $-(\text{PEA} + \text{H}_2\text{O})$ ], 1402 ( $^{1,5}\text{X}_{3\alpha''}$ ), 1386 ( $\text{Z}_{3\beta/4\alpha'}$ ), 1356 ( $\text{Z}_{3\alpha'}$ ), and 763 ( $^{1,5}\text{X}_{2\alpha}$ ). The two fragments at  $m/z$  654 and 622 marked with asterisks are believed to be Hex<sub>2</sub>Hep(PEA) fragments arising from two bond cleavages. The octasaccharide structure is illustrated with 4,8-anhydro-KDO at the reducing terminus as an example of one of the possible anhydro-KDO forms presumed to exist in the Hib A2 oligosaccharide structures.

parent ions for collision-induced dissociation (CID). Initially, MS/MS analysis was performed on the  $(\text{M} - \text{H})^-$  1566.5 species (Figure 4). Fragment ions present in the spectrum and shown on the octasaccharide structure are labeled according to the carbohydrate fragmentation nomenclature proposed by Domon and Costello (1988). This nomenclature defines reducing-terminal (X, Y, and Z) and nonreducing-

terminal (A, B, and C) fragments, which include both glycosidic bond (Y, Z, B, and C) and ring (A and X) cleavages. In the MS/MS spectrum, a series of reducing-terminal Y-type sequence ions ( $m/z$  1404, 1242, 1374, and 735) defines a structure with two Hex→Hex disaccharide branches located on the first two heptoses of a Hep<sub>3</sub> core. The Y ion at  $m/z$  1374 (loss of Hep from the molecular ion) and the intense B



and C ions at  $m/z$  830 and 848 fix the location of the PEA group on the middle heptose. From methylation analysis of column fractions 80–81 (Table V), it was established that the Hex→Hex disaccharides must both be Glc1→4Glc1→moieties, allowing for the following overall structure:



It would appear that the presence of the PEA group directs the fragmentation of the molecule to give abundant nonreducing-terminal fragment ions. In addition to the B and C ions arising from glycosidic bond cleavage between the first and middle heptoses, an intense B ion at  $m/z$  1346 represents loss of the reducing-terminal anhydro-KDO. The ion at  $m/z$  506 is tentatively assigned as an  $^{2,4}\text{A}$  ion arising from cleavage of the C<sub>2</sub>–C<sub>3</sub> and C<sub>4</sub>–C<sub>5</sub> bonds of the middle heptose. As this fragment appears to contain the PEA moiety, the ion suggests that the PEA group is linked to the 4-position of the middle heptose. The same fragment was not seen in the MS/MS spectrum of the dephosphorylated octasaccharide (data not shown).

Other components of the oligosaccharide mixture were also analyzed by MS/MS. In all cases, the B and C ions representing glycosidic bond cleavages between the first and middle heptoses were useful for establishing the relative sizes of the nonreducing-terminal branches. For example, the MS/MS spectrum of the hexasaccharide at  $m/z$  1242.4 contained increase B and C ions at  $m/z$  506 and 524, suggesting that the middle heptose is not substituted with hexoses. Rather, the Hex→Hex branch present on that structure is located on the heptose bound to the anhydro-KDO. Coupled with the methylation analysis data for Bio-Gel P-4 column fractions 88–89 (see Table V), this result indicates that the heptose bound to the anhydro-KDO is the 1,3,4-linked heptose, as was the case in the hexasaccharide from *H. influenzae* nontypable strain 2019 (Phillips et al., 1992). The parent ion at  $m/z$  1890.6 (6 Hex, 3 Hep, 1 anhydro-KDO, and 1 PEA) was also analyzed by MS/MS and gave a spectrum with the analogous B and C ions at  $m/z$  992 and 1010, respectively. In this case, the fragments suggest a decasaccharide structure with two Hex→Hex→Hex branches on the two trlinked heptoses. Methylation analysis of fractions 71–72 (see Table V) suggested that these branches may end in terminal Gal, although the data are not conclusive.

Structures larger than the  $M_r$  1891.6 species proved unsuitable for MS/MS analysis as underivatized carbohydrates due to their low molecular ion abundances. To obtain preliminary sequence information on the  $M_r$  1932.7 component, pooled fractions 67–68 were dephosphorylated and reacted with butyl phenylhydrazine (BPH) to produce reducing-terminal hydrazino derivatives (John & Gibson, 1990). Reverse-phase HPLC separation of the reaction mixture produced three main peaks, typical of anhydro-KDO-containing oligosaccharides, which generally give multiple isobaric reaction products (Melaugh et al., 1992; Phillips et al., 1992). When analyzed by LSIMS, all three peaks contained a mixture of the same two main components:  $M_r$  2076.9 (7 Hex, 3 Hep, anhydro-KDO, and BPH) and  $M_r$  1955.6 (5 Hex, 3 Hep, HexNAc, anhydro-KDO, and BPH). Two series of fragment ions, which eventually converged to a single series, were

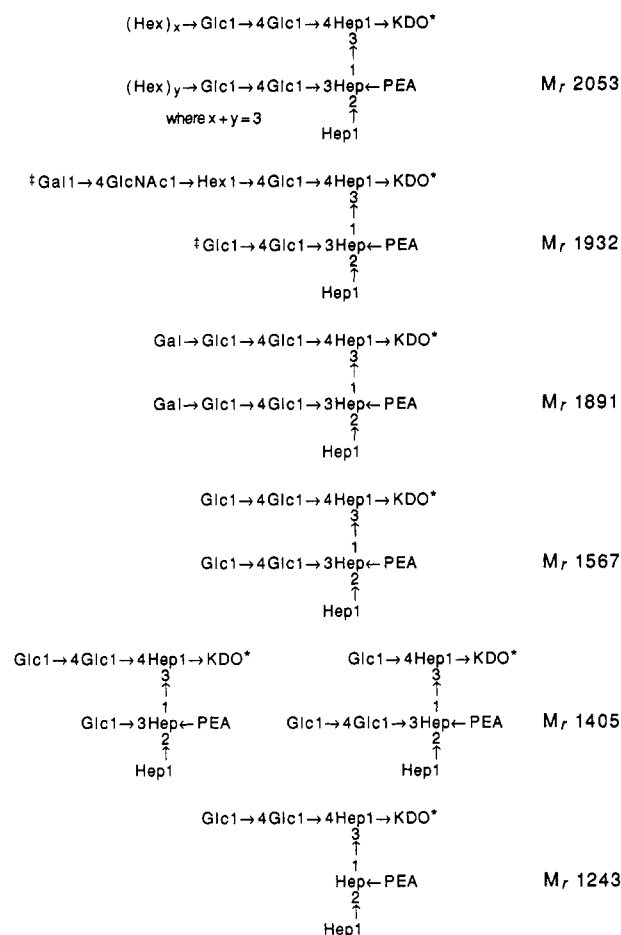


FIGURE 5: Partial structures of several oligosaccharides present in the *H. influenzae* A2 LOS sample. Two isobaric structures were assigned to the  $M_r$  1405 component on the basis of MS/MS analysis. The  $M_r$  2053 and 1891 structures, which contain only hexoses as branch sugars, were tentatively assigned the core structure of the  $M_r$  1567 component, with the identities of other branch sugars uncertain. The branching pattern of the  $M_r$  1891 component was established by MS/MS analysis, while insufficient information was available to unambiguously determine the relative sizes of the two branches on the  $M_r$  2053 component. On the basis of methylation analysis data and LSIMS fragment ions, the  $M_r$  1932 component was tentatively assigned the structure shown, which is likely to contain terminal lactosamine. It is not clear whether this structure contains the  $M_r$  1567 core or not. The Hex substituted with the Gal→GlcNAc→ moiety may be either Gal or Glc, and \* indicates that the two branches may be interchanged.

apparent in these spectra. Specifically, ions at  $m/z$  1913, 1751, 1589, 1427, and 1265 could be assigned as five sequential losses of hexose ( $-162 \text{ Da/Hex}$ ) from the  $(M - H)^-$  ion at 2075.9, and ions at  $m/z$  1792, 1589, 1427, and 1265 could be assigned as sequential losses of Hex, HexNAc, Hex, and Hex from the  $(M - H)^-$  ion at 1954.6. Because the two ion series overlap, it is not clear whether ions below the  $m/z$  1589 fragment arise from one or both of the molecular ions. However, the data suggest that at least one of the structures must contain a large branch and a Hex→Hex branch, whose relative positions could not be established. Figure 5 depicts the set of partial oligosaccharide structures determined by LSIMS, MS/MS, composition, and methylation analyses.

## DISCUSSION

Our structural studies of the LOS from Hib strain A2 focused on examining the O-deacylated LOS preparation as a heterogeneous mixture and working with semipurified



oligosaccharide and Lipid A fractions derived from acid hydrolysis of the LOS. Initial ESMS analysis of the "intact" A2 LOS mixture after only O-deacylation readily established several basic features of the LOS population, such as the number of components present, their molecular weights, and their structural homology. As the electrospray mass spectrum did not show any of the artifacts and extra heterogeneity known to be introduced into the oligosaccharide and Lipid A fractions by the acid hydrolysis step, it also provided a means of accounting for acid-labile moieties such as sialic acid, phosphate linked to the 4-position of KDO, and reducing-terminal phosphate on the Lipid A. The 11 components detected in the spectrum were all shown by mass difference to be related to one another by the addition or deletion of monosaccharides and PEA. No heterogeneity was associated with the O-deacylated Lipid A group, which was present only as a diphosphorylated species.

While nine of the 11 O-deacylated LOS structures contained only hexose residues extending from the heptose trisaccharide core region, two components appeared to be unique structures containing HexNAc and sialic acid. Neuraminidase treatment of the O-deacylated LOS mixture resulted in the removal of a moiety with the residue mass of sialic acid (calculated  $\Delta$  291.3 Da) from these latter two components and did not alter any of the other species present in the mixture. Sialic acid has been detected in the LOS of several mucosal pathogens (Gibson et al., 1993; Mandrell et al., 1991, 1992), where it is believed to be attached to the galactose residue of a terminal lactosamine moiety. Hib strain A2 LOS was previously found to contain about 0.4% sialic acid by weight (Mandrell et al., 1992), and experiments with neuraminidase suggested that only a single 3.7-kDa band on SDS-polyacrylamide gels was sialylated. Based on ESMS peak heights, our results suggest that the two sialylated components ( $M_r$  3256.2 and 3416.4) constitute roughly 5 mol % of the O-deacylated A2 LOS mixture, assuming that all components of the mixture ionize equally well. This translates into  $\approx 0.5\%$  sialic acid by weight in the O-deacylated LOS mixture and  $\approx 0.4\%$  by weight in the intact LOS sample. While Mandrell et al. (1992) estimated the  $M_r$  of the sialylated component to be about 3.7 kDa by SDS-PAGE analysis, our ESMS results indicate that the two highest molecular weight components of the A2 LOS mixture (calculated  $M_r$  4131.4 and 4293.6) are actually the sialylated species, with the  $M_r$  4131.4 component being the more abundant of the two. It is possible that these LOS run relatively fast on SDS-PAGE due to the presence of the sialic acid residue.

Mandrell et al. (1992) also demonstrated that after the immobilized 3.7-kDa LOS was treated with neuraminidase, it bound MAb 3F11, a MAb which recognizes human glycosphingolipids possessing terminal Gal $\beta$ 1 $\rightarrow$ 4GlcNAc structures (Mandrell et al., 1988). This epitope also occurs in the LOS from *N. gonorrhoeae* (Yamasaki et al., 1991a,b), *N. meningitidis* (Mandrell et al., 1991), and *H. ducreyi* (Melaugh et al., 1992) and has been described as a potential acceptor for LOS sialylation (Mandrell et al., 1990). In both its sialylated and asialo forms, terminal lactosamine on LOS structures may enable pathogenic bacteria to better evade host defense mechanisms through host mimicry. Our ESMS results indicated that in the case of Hib A2 LOS, sialylation occurs exclusively on components containing HexNAc. While these species were minor components in the mixture studied, it is possible that their levels may be elevated during Hib colonization of host tissues.

The structural heterogeneity present in the O-deacylated LOS mixture was reflected in the oligosaccharide fraction obtained by mild acid hydrolysis of the LOS. Oligosaccharides from all of the species represented in the O-deacylated LOS mixture were detected in the hydrolyzed sample, with the two sialylated structures being recovered in their asialo forms. Of the many components observed, the major component was a triantennary octasaccharide of  $M_r$  1567.5. This species contained a Hep<sub>3</sub>(anhydro-KDO) core with two Glc1 $\rightarrow$ 4Glc1 $\rightarrow$  branches and a single PEA group. Methylation analysis and tandem mass spectral data showed that extension of both disaccharide branches occurs in the higher molecular weight components of the mixture. Composition analysis, methylation analysis, and LSIMS fragmentation of a hydrazino derivative of the dephosphorylated  $M_r$  1932.7 component indicated that it is likely to contain a terminal Gal1 $\rightarrow$ 4GlcNAc $\rightarrow$  disaccharide, making it the likely acceptor for sialylation. Given that this terminal lactosamine is built off a hexose disaccharide, it is possible that the entire lacto-*N*-neotetraose structure exists, as has been observed in gonococcal (John et al., 1991; Yamasaki et al., 1991a) and meningococcal LOS (Gamian et al., 1992; Jennings et al., 1983; Michon et al., 1990).

Although some components of the Hib A2 oligosaccharide mixture were previously found as minor components in the oligosaccharides from *H. influenzae* nontypable strain 2019, the major components representative of the two strains differed in several important ways. Oligosaccharides from the nontypable strain contained predominantly 2 PEAs and had a lactose moiety (Gal $\beta$ 1 $\rightarrow$ 4Glc $\beta$ 1 $\rightarrow$ ) attached to the first heptose, rather than a glucose disaccharide. Additionally, the oligosaccharides from Hib A2 were triantennary and contained a larger percentage of higher molecular weight components than the corresponding preparation from the nontypable strain. The significance of these structural differences is not clear, although it has been observed that Hib strains which express higher molecular weight structures have "full virulence" (Kimura & Hansen, 1986). Additionally, while the O-deacylated LOS mixture from Hib A2 contained two minor high molecular weight species that were quantitatively sialylated, no evidence for sialylated structures was seen in the corresponding electrospray spectrum from the nontypable strain 2019 (Gibson et al., 1993).

The production of LOS with more highly branched oligosaccharide structures may offer Hib added flexibility in evading host defense mechanisms. Additionally, the propensity of many Hib LOS epitopes to undergo rapid phase variation (Kimura & Hansen, 1986; Kimura et al., 1987; Weiser et al., 1989) may increase the odds of successful colonization of host tissues. As the ESMS methodology is further refined to allow processing and analysis of microscale samples, it is possible that LOS samples from clinical isolates could eventually be studied, offering a means of evaluating LOS heterogeneity and phase variation in vivo. Genetic studies have begun to reveal the subtleties of LOS epitope expression (McLaughlin et al., 1992), suggesting that phase-varying epitopes may be separated from stable carbohydrate epitopes in the LOS structure. While our preliminary structural studies are consistent with this emerging picture of Hib LOS, complete structural characterization of important LOS epitopes is required to correlate LOS structure with epitope expression and pathogenesis.

## ACKNOWLEDGMENT

We would like to acknowledge the technical assistance of L. Reinders and D. Tang, and we thank W. Melaugh for valuable contributions to these studies.

## REFERENCES

- Auzanneau, F.-I., Charon, D., & Szabó, L. (1991) *J. Chem. Soc., Perkin Trans. 1*, 509–517.
- Campagnari, A. A., Gupta, M. R., Dudas, K. C., Murphy, T. F., & Apicella, M. A. (1987) *Infect. Immun.* 55, 882–887.
- Campagnari, A. A., Spinola, S. M., Lesse, A. J., Abu Kwaik, Y., Mandrell, R. E., & Apicella, M. A. (1990) *Microb. Pathogen.* 8, 353–362.
- Cope, L. D., Yogev, R., Mertsola, J., Argyle, J. C., McCracken, G. H., Jr., & Hansen, E. J. (1990) *Infect. Immun.* 58, 2343–2351.
- Darveau, R. P., & Hancock, R. E. W. (1983) *J. Bacteriol.* 155, 831–838.
- Domon, B., & Costello, C. E. (1988) *Glyconjugate J.* 5, 397–409.
- Falick, A. M., Wang, G. H., & Walls, F. C. (1986) *Anal. Chem.* 58, 1308–1311.
- Flesher, A. R., & Insel, R. A. (1978) *J. Infect. Dis.* 138, 719–730.
- Gamian, A., Beurret, M., Michon, F., Brisson, J.-R., & Jennings, H. J. (1992) *J. Biol. Chem.* 267, 922–925.
- Gibson, B. W., Melaugh, W., Phillips, N. J., Apicella, M. A., Campagnari, A. A., & Griffiss, J. M. (1993) *J. Bacteriol.* (submitted for publication).
- Gilsdorf, J. R., & Ferrieri, P. (1986) *J. Infect. Dis.* 153, 223–231.
- Hardy, M. R., Townsend, R. R., & Lee, Y. C. (1988) *Anal. Biochem.* 170, 54–62.
- Helander, I. M., Lindner, B., Brade, H., Altmann, K., Lindberg, A. A., Rietschel, E. T., & Zähringer, U. (1988) *Eur. J. Biochem.* 177, 483–492.
- Inzana, T. J. (1983) *J. Infect. Dis.* 148, 492–499.
- Inzana, T. J., Seifert, W. E., Jr., & Williams, R. P. (1985) *Infect. Immun.* 48, 324–330.
- Jennings, H. J., Johnson, K. G., & Kenne, L. (1983) *Carbohydr. Res.* 121, 233–241.
- John, C. M., & Gibson, B. W. (1990) *Anal. Biochem.* 187, 281–291.
- John, C. M., Griffiss, J. M., Apicella, M. A., Mandrell, R. E., & Gibson, B. W. (1991) *J. Biol. Chem.* 266, 19303–19311.
- Kimura, A., & Hansen, E. J. (1986) *Infect. Immun.* 51, 69–79.
- Kimura, A., Patrick, C. C., Miller, E. E., Cope, L. D., McCracken, G. H., Jr., & Hansen, E. J. (1987) *Infect. Immun.* 55, 1979–1986.
- Larson, G., Karlsson, H., Hansson, G. C., & Pimlott, W. (1987) *Carbohydr. Res.* 161, 281–290.
- Leverly, S. B., & Hakomori, S.-I. (1987) in *Methods in Enzymology* (Ginsburg, V., Ed.) Vol. 138, pp 13–25, Academic Press, New York.
- Mandrell, R. E., Griffiss, J. M., & Macher, B. A. (1988) *J. Exp. Med.* 168, 107–126.
- Mandrell, R. E., Lesse, A. J., Sugai, J. V., Shero, M., Griffiss, J. M., Cole, J. A., Parsons, N. J., Smith, H., Morse, S. A., & Apicella, M. A. (1990) *J. Exp. Med.* 171, 1649–1664.
- Mandrell, R. E., Kim, J. J., John, C. M., Gibson, B. W., Sugai, J. V., Apicella, M. A., Griffiss, J. M., & Yamasaki, R. (1991) *J. Bacteriol.* 173, 2823–2832.
- Mandrell, R. E., McLaughlin, R., Abu Kwaik, Y., Lesse, A., Yamasaki, R., Gibson, B., Spinola, S. M., & Apicella, M. A. (1992) *Infect. Immun.* 60, 1322–1328.
- McLaughlin, R., Spinola, S. M., & Apicella, M. A. (1992) *J. Bacteriol.* 174, 6455–6459.
- Melaugh, W., Phillips, N. J., Campagnari, A. A., Karalus, R., & Gibson, B. W. (1992) *J. Biol. Chem.* 267, 13434–13439.
- Michon, F., Beurret, M., Gamian, A., Brisson, J.-R., & Jennings, H. J. (1990) *J. Biol. Chem.* 265, 7243–7247.
- Moxon, E. R. (1990) in *Principles and Practice of Infectious Diseases* (Mandell, G. L., Douglas, J. R. G., & Bennett, J. E., Eds.) pp 1722–1729, Churchill Livingstone Inc., New York.
- Parr, T. R., Jr., & Bryan, L. E. (1984) *Can. J. Microbiol.* 30, 1184–1187.
- Patrick, C. C., Kimura, A., Jackson, M. A., Hermanstorfer, L., Hood, A., McCracken, G. H., Jr., & Hansen, E. J. (1987) *Infect. Immun.* 55, 2902–2911.
- Patrick, C. C., Pelzel, S. E., Miller, E. E., Haanes-Fritz, E., Radolf, J. D., Gulig, P. A., McCracken, G. H., Jr., & Hansen, E. J. (1989) *Infect. Immun.* 57, 1971–1978.
- Phillips, N. J., John, C. M., Reinders, L. G., Gibson, B. W., Apicella, M. A., & Griffiss, J. M. (1990) *Biomed. Environ. Mass Spectrom.* 19, 731–745.
- Phillips, N. J., Apicella, M. A., Griffiss, J. M., & Gibson, B. W. (1992) *Biochemistry* 31, 4515–4526.
- Spinola, S. M., Abu Kwaik, Y., Lesse, A. J., Campagnari, A. A., & Apicella, M. A. (1990) *Infect. Immun.* 58, 1558–1564.
- Stellner, K., Saito, H., & Hakomori, S.-I. (1973) *Arch. Biochem. Biophys.* 155, 464–472.
- Turk, D. C. (1982) in *Haemophilus influenzae, epidemiology, immunology, and prevention of disease* (Sell, S. H., & Wright, P. F., Eds.) pp 1–9, Elsevier, Amsterdam.
- van Alphen, L., Klein, M., Geelen-van den Broek, L., Riemens, T., Eijk, P., & Kamerling, J. P. (1990) *J. Infect. Dis.* 162, 659–663.
- Virji, M., Weiser, J. N., Lindberg, A. A., & Moxon, E. R. (1990) *Microb. Pathogen.* 9, 441–450.
- Walls, F. C., Baldwin, M. A., Falick, A. M., Gibson, B. W., Kaur, S., Maltby, D. A., Gillece-Castro, B. L., Medzihradsky, K. F., Evans, S., & Burlingame, A. L. (1990) in *Biological Mass Spectrometry* (Burlingame, A. L., & McCloskey, J. A., Eds.) pp 197–216, Elsevier, Amsterdam.
- Weiser, J. N., Love, J., & Moxon, E. R. (1989) *Cell* 59, 657–665.
- Yamasaki, R., Bacon, B. E., Nasholds, W., Schneider, H., & Griffiss, J. M. (1991a) *Biochemistry* 30, 10566–10575.
- Yamasaki, R., Nasholds, W., Schneider, H., & Apicella, M. (1991b) *Mol. Immunol.* 28, 1233–1242.
- Zamze, S. E., & Moxon, E. R. (1987) *J. Gen. Microbiol.* 133, 1443–1451.